nature photonics

ARTICLES

PUBLISHED ONLINE: 9 MAY 2016 | DOI: 10.1038/NPHOTON.2016.73

Optomechanically induced stochastic resonance and chaos transfer between optical fields

Faraz Monifi[1†], Jing Zhang[1,2,3*], Şahin Kaya Özdemir[1*], Bo Peng[1†], Yu-xi Liu[3,4], Fang Bo[1,5], Franco Nori[6,7] and Lan Yang[1*]

Chaotic dynamics has been reported in many physical systems and has affected almost every field of science. Chaos involves hypersensitivity to the initial conditions of a system and introduces unpredictability into its output. Thus, it is often unwanted. Interestingly, the very same features make chaos a powerful tool to suppress decoherence, achieve secure communication and replace background noise in stochastic resonance—a counterintuitive concept that a system's ability to transfer information can be coherently amplified by adding noise. Here, we report the first demonstration of chaos-induced stochastic resonance in an optomechanical system, as well as the optomechanically mediated chaos transfer between two optical fields such that they follow the same route to chaos. These results will contribute to the understanding of nonlinear phenomena and chaos in optomechanical systems, and may find applications in the chaotic transfer of information and for improving the detection of otherwise undetectable signals in optomechanical systems.

Advances in micro- and nanofabrication technologies have enabled the creation of novel structures in which enhanced light–matter interactions result in mechanical deformations and self-induced oscillations via the radiation pressure of photons. Suspended mirrors[1,2], whispering-gallery-mode (WGM) microresonators (for example, microtoroids[3,4], microspheres[5–7] and microdisks[8–10]), cavities with a membrane in the middle[11] and photonic-crystal zipper cavities[12] are examples of such optomechanical systems where the coupling between optical and mechanical modes has been observed. These have opened new possibilities for fundamental and applied research. For example, they have been proposed for preparing non-classical states of light[13,14], high-precision metrology[15,16], phonon lasing[17–19] and cooling to their ground state[20–22]. The nonlinear dynamics originating from the coupling between the optical and mechanical modes of an optomechanical resonator can cause both the optical and the mechanical modes to evolve from periodic to chaotic oscillations. These can find use in applications such as random number generation and secure communication[23,24], as well as chaotic optical sensing[25]. In addition, the intrinsic chaotic dynamics of a nonlinear system can replace the stochastic process (conventionally an externally provided Gaussian noise) required for stochastic resonance[26]: a phenomenon in which the presence of noise optimizes the response of a nonlinear system, leading to the detection of weak signals. Stochastic resonance[26,27] is encountered in bistable systems, where noise induces transitions between two locally stable states enhancing the system's response to a weak external signal. A related effect showing the constructive role of noise is coherence resonance[28], which is defined as stochastic resonance without an external signal. Both stochastic resonance[26,27,29–37] and coherence resonance[28,38–45] are known to occur in a wide range of physical and biological systems, including electronics[28,31,45], lasers[35,39–41], superconducting quantum interference devices[32], sensory neurons[27,29,33], nanomechanical oscillators[34] and exciton–polaritons[37]. However, to date, they have not been reported in an optomechanical system. In this Article, we demonstrate chaos-mediated stochastic resonance in an optomechanical microresonator.

Despite recent progress and interest in the nonlinear dynamics involved, optomechanical chaos remains largely unexplored experimentally. Further experimental and theoretical studies on chaos and stochastic resonance in optomechanical systems could substantially advance the field and may be useful for high-precision measurements and for fundamental tests of nonlinear dynamics. Here, we report the demonstration of optomechanically mediated transfer of chaos from a strong optical field (pump) that excites mechanical oscillations, to a very weak optical field (probe) in the same resonator. We show that when the pump power is increased, the probe and pump fields follow the same route from periodic to quasi-periodic oscillations and finally to chaotic oscillations. Chaos transfer from the pump to the probe is mediated by the mechanical motion of the resonator, because there is no direct talk between these two largely detuned optical fields. Moreover, we report the first observation of stochastic resonance in an optomechanical system. The required stochastic process is provided by the intrinsic chaotic dynamics and optomechanical backaction.

Optical chaos in an optomechanical resonator

Our experimental system was composed of a fibre-taper-coupled WGM microtoroid resonator (Fig. 1a; Supplementary Section A). Light from an external cavity laser in the 1,550 nm band is first amplified by an erbium-doped fibre amplifier (EDFA) and then coupled into a microtoroid to act as the pump for excitation of mechanical modes. The optical transmission spectrum, obtained by scanning the wavelength of the pump laser, shows a typical Lorentzian lineshape with a low-power pump field (Fig. 1b). The

[1]Department of Electrical and Systems Engineering, Washington University, St Louis, Missouri 63130, USA. [2]Department of Automation, Tsinghua University, Beijing 100084, China. [3]Center for Quantum Information Science and Technology, TNList, Beijing 100084, China. [4]Institute of Microelectronics, Tsinghua University, Beijing 100084, China. [5]The MOE Key Laboratory of Weak Light Nonlinear Photonics, TEDA Applied Physics Institute and School of Physics, Nankai University, Tianjin 300457, China. [6]CEMS, RIKEN, Saitama 351-0198, Japan. [7]Physics Department, The University of Michigan, Ann Arbor, Michigan 48109-1040, USA. †Present addresses: Department of Electrical and Computer Engineering, University of California, San Diego La Jolla, California 92093-0407, USA (F.M.); IBM Thomas J. Watson Research Center, Yorktown Heights, New York 10598, USA (B.P.). *e-mail: ozdemir@wustl.edu; jing-zhang@mail.tsinghua.edu.cn; yang@seas.wustl.edu

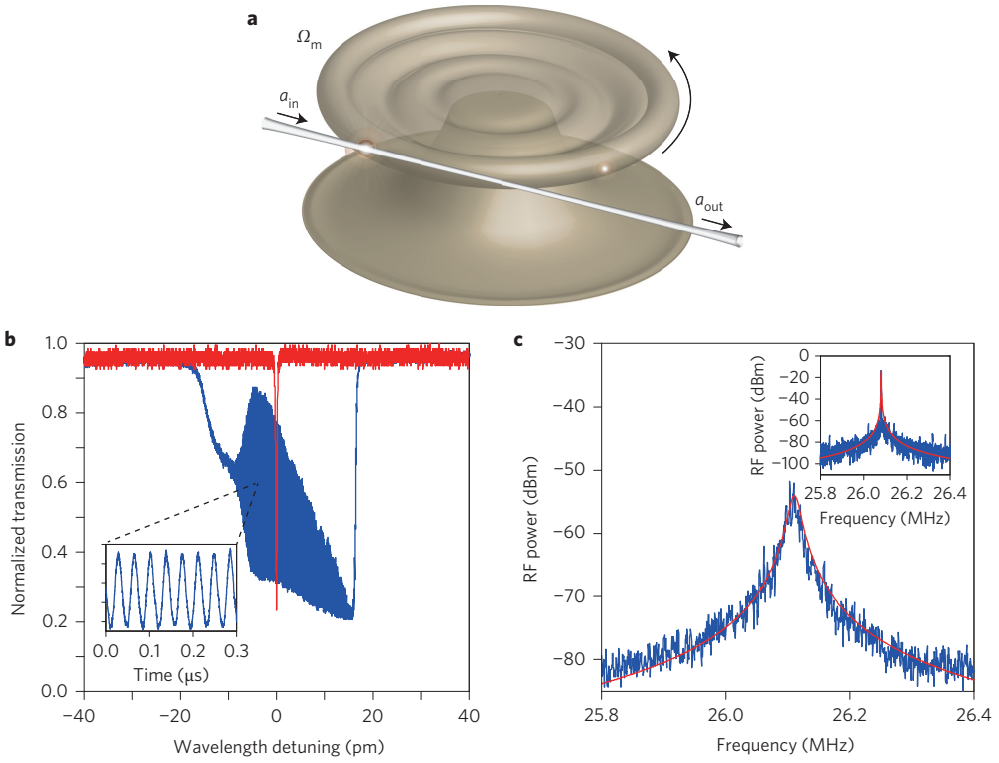

Figure 1 | Whispering-gallery-mode microtoroid optomechanical resonator. a, Sectional view of the microtoroid illustrating the mechanical motion induced by the optical radiation force. **b**, Typical transmission spectra obtained by scanning the wavelength of a tunable laser with a power well below (red) and above (blue) the mechanical oscillation threshold. At high powers (blue), thermally induced linewidth broadening and fluctuations due to the mechanical oscillations kick in. Inset: Close-up view of the fluctuations in the transmission, obtained at a specific wavelength of the laser, revealing a sinusoidal oscillation at the frequency Ω_m of the mechanical oscillation. **c**, Typical electrical spectrum analyser trace of the detected photocurrent below the mechanical oscillation threshold. Inset: The spectrum above threshold. Blue traces, experimental data; red curves, best fitting curve. RF, radiofrequency.

quality factor of this optical mode is 1×10^7. As the pump power increases, the spectrum changes from a Lorentzian lineshape to a distorted asymmetric lineshape as a result of thermal nonlinearity[46,47]. This helps to keep the pump laser blue-detuned with respect to the resonant line of the microcavity. As a result, radiation-pressure-induced mechanical oscillations take place, leading to modulation of the transmitted light at the frequency of the mechanical motion (Fig. 1b, inset). This is reflected by the oscillations imprinted on the optical transmission spectra (Fig. 1b). Radiofrequency (RF) power versus frequency traces, obtained using an electrical spectrum analyser (ESA), revealed a Lorentzian spectrum located at $\Omega_m \approx 26.1$ MHz with a linewidth of ~200 kHz, giving a mechanical quality factor of $Q_m \approx 131$ when the pump power is below the threshold of mechanical oscillation (Fig. 1c). For powers above threshold, linewidth narrowing is clearly observed (Fig. 1c, inset).

To investigate the effect of mechanical motion induced by the strong pump field on a weak light field (probe light) within the same resonator, we used an external cavity laser with emission in the 980 nm band. The power of the probe laser was chosen such that it did not induce any thermal or mechanical effect on the resonator; that is, its power was well below the threshold of mechanical oscillations. We monitored the transmission spectra of the pump and the probe fields separately by photodiodes connected to an oscilloscope and an ESA. The probe resonance mode had a quality factor of 6×10^6.

As we increase the power of the pump field, the transmitted pump light is observed to transit from a fixed state to a region of periodic oscillations and finally to the chaotic regime through period-doubling bifurcation[48,49] cascades (Fig. 2a). A periodic regime, with only a few sharp peaks, then a quasi-periodic regime, with infinite discrete sharp peaks, are observed successively in the output spectrum of the pump field (Supplementary Section B). Finally, the whole baseline of the output spectrum of the pump field increases, suggesting that the system has entered the chaotic regime. All these results agree very well with those of previous studies[4,48,49]. These phenomena observed for the pump field originate from nonlinear optomechanical coupling between the optical pump field and the mechanical mode of the resonator. Intuitively, one may attribute this observed dynamics to the chaotic mechanical motion of the resonator[50]. However, the mechanical motion of the resonator, reconstructed using the experimental data in the theoretical model, shows that the optical signal is chaotic even if the mechanical motion of the resonator is periodic (Supplementary Section E). Thus, we conclude that the reason for the chaotic behaviour in the optical field in our experiments is a strong nonlinear optical Kerr response induced by nonlinear coupling between the optical and mechanical modes.

By simultaneously monitoring the probe field we found that, as the pump power increases, the probe also experiences periodic, quasi-periodic and finally chaotic regimes (Supplementary Section C). More importantly, the pump and probe enter the chaotic regime via the same bifurcation route (Fig. 2); that is, both optical fields experience the same number of period-doubling cascades and the doubling points occur at the same values of pump power. These features are clearly seen in the phase-space plots in Fig. 2a,b and in the bifurcation diagrams in Fig. 2c,d. The experimental data fit very well with the bifurcation theory. Each periodic region is smaller than the previous region by a factor $a_1/a_2 = 4.5556$ for the pump and $\tilde{a}_1/\tilde{a}_2 = 4.5556$ for the probe, and these factors are close to the first universal Feigenbaum constant of 4.6692. The ratio between the width of a tine and the width of one of its two subtines for the pump is $b_1/b_2 = 2.6412$ and that for the probe is $\tilde{b}_1/\tilde{b}_2 = 2.8687$,

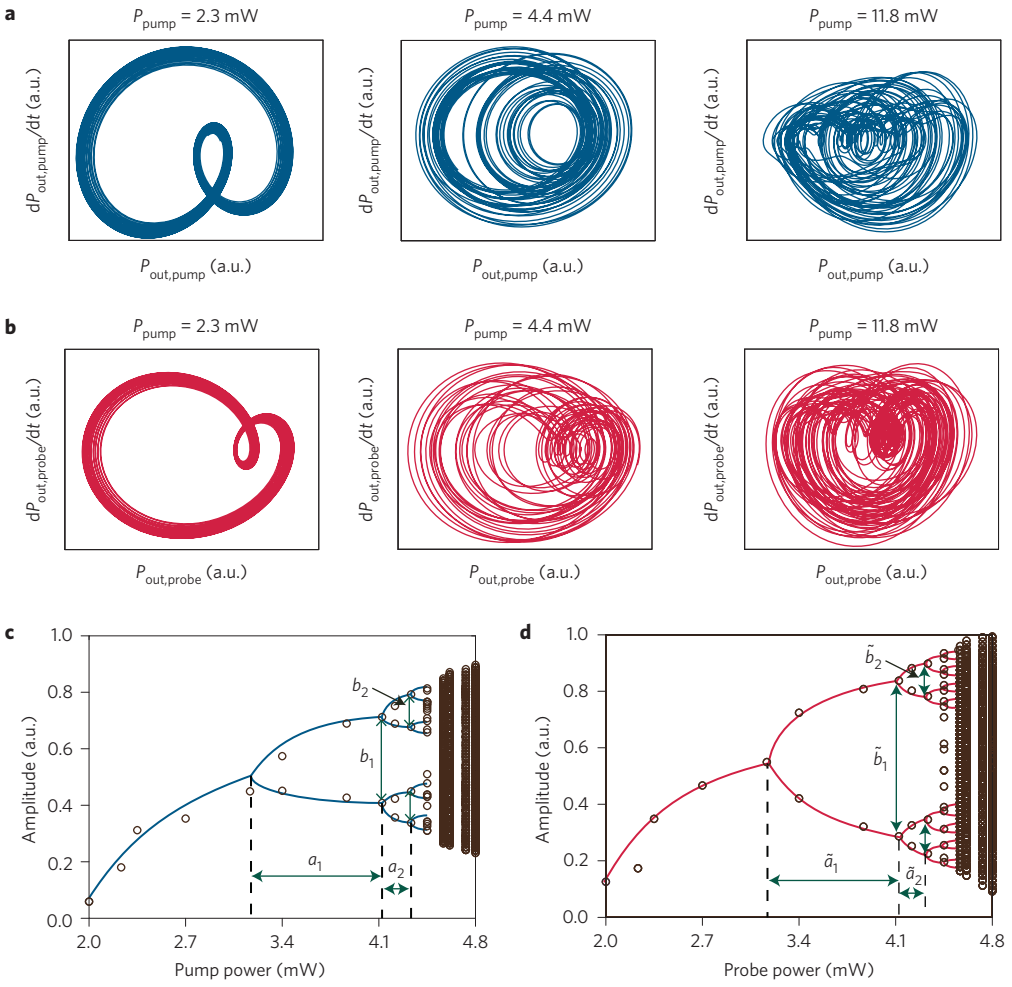

Figure 2 | Optomechanically mediated chaos generation and transfer between optical fields. a,**b**, Phase diagrams of the pump (**a**) and probe (**b**) fields in periodic (left), quasi-periodic (middle) and chaotic (right) regimes. The phase diagrams were obtained by plotting the first time derivative of the measured output power of the pump (**a**) and the probe (**b**) fields as a function of the respective output powers. **c**,**d**, Bifurcation diagrams of the pump (**c**) and probe (**d**) fields as a function of input pump power. The pump and probe enter the chaotic regime via the same bifurcation route. The ratios of the bifurcation intervals for the pump (a_1/a_2) and probe ($\tilde{a}_1/\tilde{a}_2$) are both 4.5556. The ratio between the width of a tine and the width of one of its two subtines is $b_1/b_2 = 2.6412$ for the pump and $\tilde{b}_1/\tilde{b}_2 = 2.8687$ for the probe.

both of which are close to the second universal Feigenbaum constant, 2.5029. The probe field used in the experiments was so weak that it could not induce any mechanical oscillations of its own and the large frequency-detuning between the pump field (in the 1,550 nm band) and the probe field (in the 980 nm band) ensured that there was no direct crosstalk between the optical fields. Thus, the observed close relation between the route to chaos for the pump and probe fields can only be attributed to the fact that the periodic mechanical motion of the microresonator mediates coupling between the optical modes via optomechanically induced Kerr-like nonlinearity and enables the probe to follow the pump field (Supplementary Sections B and D).

Controlling chaos and stochastic noise

We next investigated the effects of increasing pump power (1,550 nm band) on the detected pump and probe signals (980 nm band), the degree of sensitivity to the initial conditions, and chaos in the probe. To do this, we first calculated the maximal Lyapunov exponent (MLE) from the detected pump and probe signals. Lyapunov exponents quantify the sensitivity of a system to the initial conditions and give a measure of predictability. They are a measure of the rate of convergence or divergence of nearby trajectories in phase space. The behaviour of the MLE is a good indicator of the degree of convergence or divergence of an entire system. A positive MLE implies divergence and sensitivity to initial conditions, and that the orbits are on a chaotic attractor. If, on the other hand, the MLE is negative, then the trajectories converge to a common fixed point. A zero exponent indicates that the orbits maintain their relative positions and are on a stable attractor. We observed that, with increasing pump power, the degree of chaos and sensitivity to initial conditions, as indicated by the positive MLE, first increased and then decreased after reaching its maximum, both for the pump and the probe fields (Fig. 3a). With further increase of the pump, the MLE became negative, indicating a reverse period-doubling route out of chaos into periodic dynamics. In addition to the pump power, the pump-cavity detuning and the damping rate of the pump affect the MLE for both the pump and the probe fields (Supplementary Section F).

We also measured the bandwidth D of the probe signal and found that it increased with increasing pump power (Fig. 3b–e), and the relation between D of the probe signal and the pump power P_{pump} follows the power function $D = \alpha P_{pump}^{1/2}$, with $\alpha = 1.65 \times 10^8$ Hz mW$^{-1/2}$ (Fig. 3b). This is contrary to the expectation that the less (more) chaotic the signal, the smaller (larger) its bandwidth. We attribute this to the presence of both the deterministic noise from chaos and the stochastic noise from the optomechanical backaction. The system

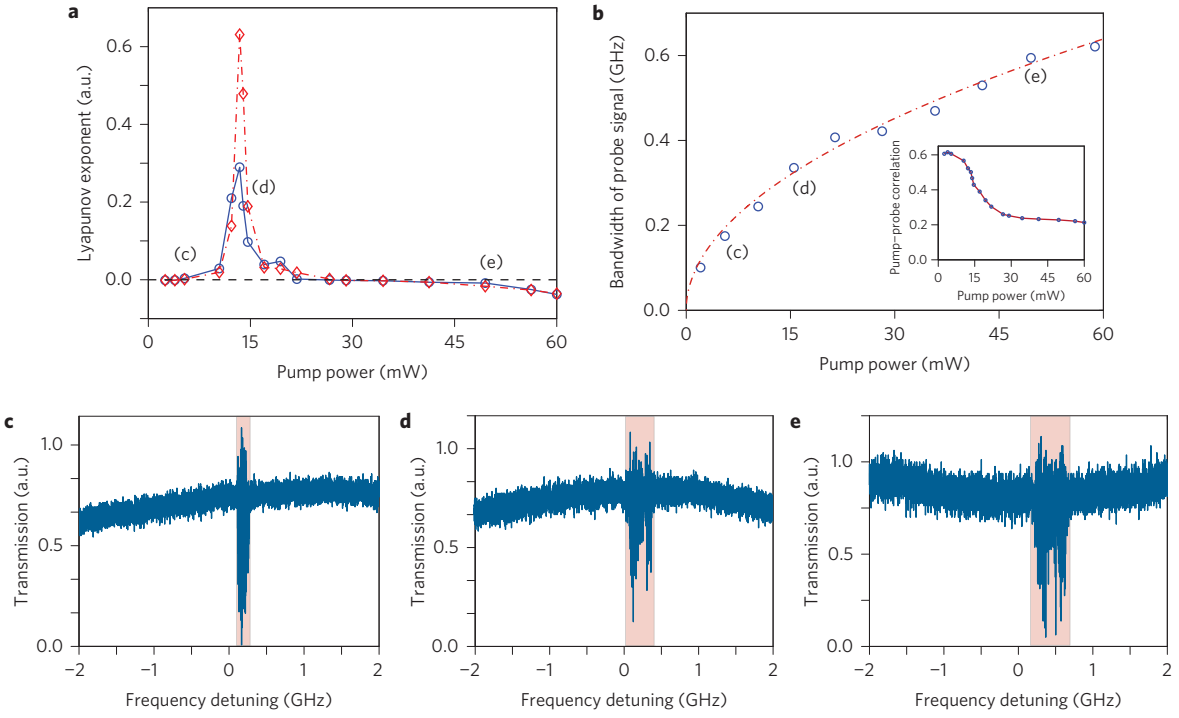

Figure 3 | Maximal Lyapunov exponents and probe bandwidth. a, Maximal Lyapunov exponents for the pump (blue) and the probe (red) fields as a function of the pump power. The Lyapunov exponents describe the sensitivity of the transmitted pump and probe signals to the input pump power. Blue circles and red diamonds are the exponents calculated from measured data. Blue and red curves are guides to the eye. **b**, Bandwidth broadening of the probe as a function of pump power. Blue circles, experimental data; red curve, fitting curve. Inset: Cross-correlation between the pump and probe fields as a function of pump power. **c**–**e**, Typical spectra obtained for the probe at different pump powers. Power increases from **c** to **e**, clearly showing the bandwidth broadening. The corresponding Lyapunov exponents and bandwidths are indicated in **a** and **b**.

is chaotic for the range of pump power where the maximal Lyapunov exponent is positive (Fig. 3a). For smaller or larger power levels, the system is not in the chaotic regime. Thus, chaos-induced noise is present only for a certain range of pump power. The effect of optomechanical backaction, on the other hand, is always present in the power range shown in Fig. 3 and its effect increases with increasing pump power. The higher the pump power, the larger the stochastic noise due to backaction (Fig. 3e has more backaction noise than Fig. 3d, which has more than Fig. 3c). In Fig. 3c,e (corresponding to zero or negative maximum Lyapunov exponent), the bandwidth is almost completely determined by the optomechanical backaction, with very small or no contribution from chaos. In Fig. 3d, the system is in the chaotic regime and thus both chaos and backaction contribute to the noise, leading to a larger probe bandwidth in Fig. 3d than in Fig. 3c. At the pump power used to obtain the spectrum shown in Fig. 3e, on the other hand, the system is no longer in the chaotic regime. However, the backaction noise reaches such high levels that it surpasses the combined effect of the chaos and backaction noises of Fig. 3d. As a result, Fig. 3e has a larger bandwidth. In our system, the pump and probe thus became less chaotic when the pump power was increased beyond a critical value. However, at the same time, their bandwidths increased, implying a greater noise contribution from the optomechanical backaction. Therefore, the correlation between the pump and probe fields decreased with increasing pump power (Fig. 3b, inset).

Stochastic resonance in an optomechanical resonator

We observed that, below a critical value, increasing the pump power increases the signal-to-noise ratio (SNR) of both the probe and the pump fields. However, beyond this value, the SNR decreases, despite increasing pump power (Fig. 4a). When the pump was turned off ($P_{\mathrm{pump}} \sim 0$ mW), the SNR of the probe signal was −10 dB. The maximum value of the SNR was obtained for a pump power of $P_{\mathrm{pump}} \sim 15$ mW. The relation between the pump power and the SNR of the probe is given by the expression $(\varepsilon/P_{\mathrm{pump}})\exp(-\beta/\sqrt{P_{\mathrm{pump}}})$, where $\varepsilon = 0.825$ mW and $\beta = 7.4764$ mW$^{1/2}$ (Supplementary Section G). Combining the relation between the bandwidth and the pump power with the relation between the SNR and pump power, we find that the relation between the SNR and the bandwidth of the probe signal scales as $\mathrm{SNR} \propto aD^{-2}\exp(-b/D)$ (Supplementary Section G). This expression indicates that the SNR is not a monotonous function of bandwidth D (that is, noise) and that it is possible to increase the SNR by increasing the noise[26,35,36]. This effect is referred to as stochastic resonance: a phenomenon in which the response of a nonlinear system to a weak input signal is optimized by the presence of a particular level of stochastic noise, that is, the noise-enhanced response of an input signal. Figure 4b provides a conceptual illustration of the mechanism leading to chaos-mediated stochastic resonance in our optomechanical system. An observed noise benefit (Fig. 4a) can be described as stochastic resonance if the input (weak signal) and output signals are well defined[27]. In our experiment, the input is given by the weak probe field (in the 980 nm band) and the output is the signal detected in the probe mode at the end of the fibre taper. In the rotated frame and with the elimination of mechanical degrees of freedom, the optical system is described by a weak periodic input (that is, the weak probe field) modulated by the frequency of the mechanical mode (Supplementary Sections B and H). The noise required for stochastic resonance can be either external or internal (due to the internal dynamics of the system). In our system it is provided by both the optomechanical backaction and chaotic dynamics, which are both controlled by the external pump field.

At low pump powers, corresponding to periodic or less-chaotic regimes (that is, a negative or zero Lyapunov exponent), the contribution of the backaction noise is small, and chaos is not strong

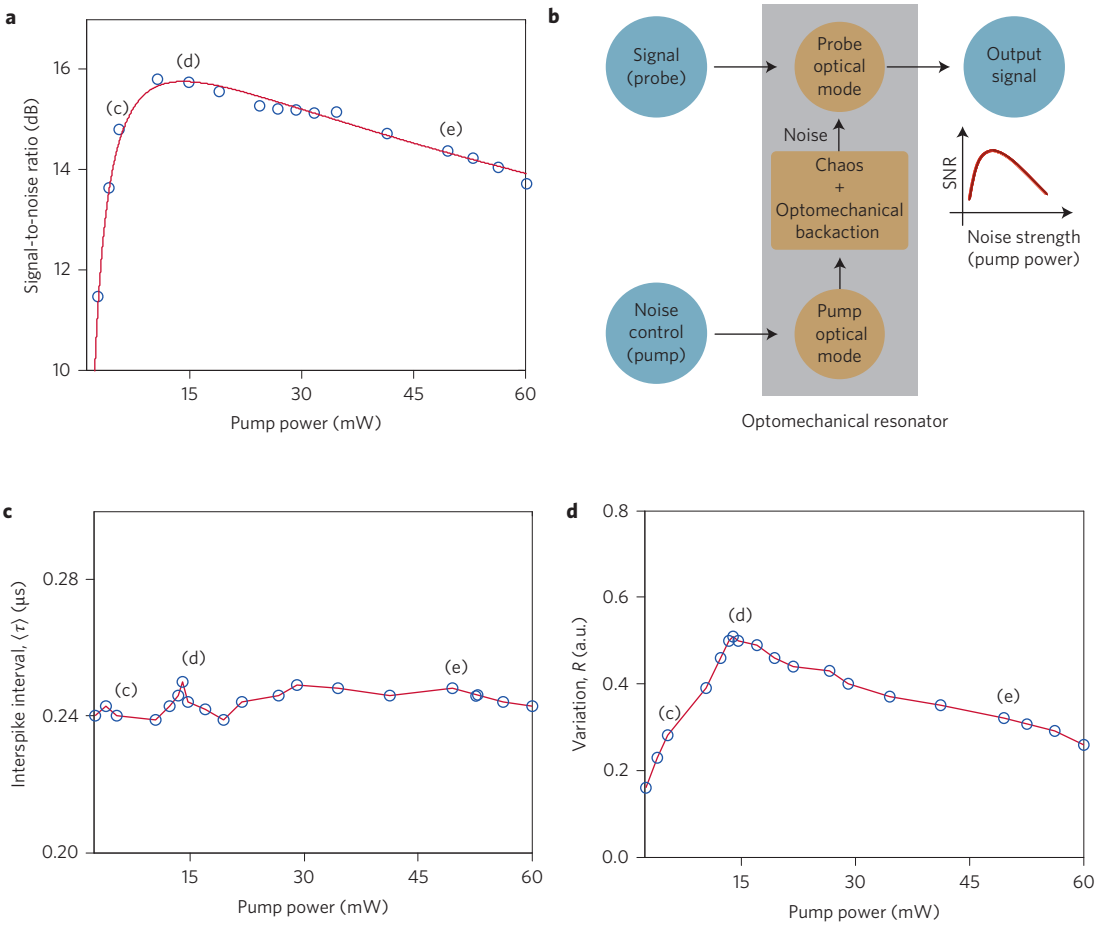

Figure 4 | Optomechanically induced chaos-mediated stochastic resonance in an optomechanical resonator. a, Signal-to-noise ratio (SNR) of the probe as a function of pump power. Solid curve: Best fit to the experimental data (open circles). **b**, Illustration conceptualizing chaos-mediated stochastic resonance in an optomechanical resonator. Mechanical motion mediates the pump–probe coupling and enables the pump field to control chaos, the strength of the optomechanical backaction, and the probe bandwidth. Hence, the pump controls the system's noise. Increasing the pump power first increases the SNR to its maximum and then reduces it. **c**,**d**, Mean $\langle\tau\rangle$ (**c**) and scaled standard deviation R (**d**) of interspike intervals τ, obtained from experimental data for the probe (blue open circles) as a function of pump power, exhibiting the theoretically expected characteristics for a system with stochastic resonance (Supplementary Section H). The data points labelled c, d and e correspond to the same points indicated in Fig. 3.

enough to amplify the signal. Therefore, the SNR is low. At much higher pump power levels, the system evolves out of chaos. At the same time, the noise contribution to the probe from the optomechanical backaction increases with increasing pump power and becomes comparable to the probe signal. Consequently, the SNR of the probe decreases. Between these two SNR minima, the noise attains the optimal level to amplify the signal coherently with the help of intermode interference due to the chaotic map, and thus an SNR maximum occurs. Indeed, resonant jumps between different attractors of a system due to chaos-mediated noise was previously suggested by Anishchenko *et al.*[30] as a route to stochastic resonance and to improve SNR.

The mean $\langle\tau\rangle$ (Fig. 4c) and scaled standard deviation $R = \sqrt{\langle\tau^2\rangle - \langle\tau\rangle^2}/\langle\tau\rangle$ (Fig. 4d) of the interspike intervals τ of the signals detected in our experiments exhibit the theoretically expected dependence on the noise (that is, pump power) for a system with stochastic resonance (Supplementary Section H). Although $\langle\tau\rangle$ is not affected by the pump power and retains its value of 0.24 μs (the resonance revival frequency of 26 MHz determined by the frequency of the mechanical mode), R attains a maximum at an optimal pump power (that is, R is a concave function of noise). On the other hand, for a system with coherence resonance, increasing noise leads to a decrease in $\langle\tau\rangle$ and R is a convex function of the noise (Supplementary Section H)[28,42,44,51]. It is known that in a system with coherence resonance the positions of the resonant peaks in the output spectra shift with increasing pump power, implying that the resonances are induced solely by noise[44]. The resonant peak in our experimentally obtained output power spectra, however, was located at the frequency of the mechanical mode, which modulated the input probe field, and its position did not change with increasing pump power (that is, noise level), providing another signature of stochastic resonance (Supplementary Section H). Thus, we believe that the observed SNR enhancement is due to the chaos-mediated stochastic resonance and hence this work constitutes the first observation of optomechanically induced chaos-mediated stochastic resonance, which is a counterintuitive process where additional noise can be helpful.

Conclusions and discussion

The ability to transfer chaos from a strong signal to a very weak signal via mechanical motion, such that the signals are correlated and follow the same route to chaos, opens new venues for applications of optomechanics. One such direction would be to transfer chaos from a classical field to a quantum field to create chaotic quantum states of light for secure and faithful transmission of quantum signals. The chaotic transfer of classical and quantum information in such cavity-optomechanical systems demonstrated here is limited by the achievable chaotic bandwidth, which is

determined by the strength of the optomechanical interaction and the bandwidth restrictions imposed by the cavity. One can increase the chaotic bandwidth by using waveguide structures that have larger bandwidths than the cavities. Moreover, the presence of chaos-mediated stochastic resonance in optomechanical systems is exciting not only for a fundamental understanding of the nonlinear dynamics induced by the optomechanical coupling, but also for the possibility of using stochastic resonance to enhance the signal-processing capabilities to detect and manipulate weak signals. Although we have performed experiments in an optomechanical system, our results can be extended to micro/nanomechanical systems where frequency-separated mechanical modes are coupled to each other, for example, acoustic modes of a micromechanical resonator[52] or cantilevers regularly spaced along a central clamped–clamped beam[53]. We believe that generating, transferring and controlling optomechanical chaos and using it for stochastic resonance paves the way for developing electronic and photonic devices that exploit the intrinsic sensitivity of chaos.

Received 16 October 2015; accepted 15 March 2016; published online 9 May 2016

References

1. Arcizet, O., Cohadon, P.-F., Briant, T., Pinard, M. & Heidman, A. Radiation-pressure cooling and optomechanical instability of a micromirror. *Nature* **444,** 71–74 (2006).
2. Gigan, S. *et al.* Self-cooling of a micromirror by radiation pressure. *Nature* **444,** 67–70 (2006).
3. Kippenberg, T. J., Rokhsari, H., Carmon, T., Scherer, A. & Vahala, K. J. Analysis of radiation-pressure induced mechanical oscillation of an optical microcavity. *Phys. Rev. Lett.* **95,** 033901 (2005).
4. Carmon, T., Rokhsari, H., Yang, L., Kippenberg, T. J. & Vahala, K. J. Temporal behavior of radiation-pressure-induced vibrations of an optical microcavity phonon mode. *Phys. Rev. Lett.* **94,** 223902 (2005).
5. Park, Y.-S. & Wang, H. Resolved-sideband and cryogenic cooling of an optomechanical resonator. *Nature Phys.* **5,** 489–493 (2009).
6. Dong, C., Fiore, V., Kuzyk, M. C. & Wang, H. Optomechanical dark mode. *Science* **338,** 1609–1613 (2012).
7. Tomes, M. & Carmon, T. Photonic micro-electromechanical systems vibrating at X-band (11-GHz) rates. *Phys. Rev. Lett.* **102,** 113601 (2009).
8. Hofer, J., Schliesser, A. & Kippenberg, T. J. Cavity optomechanics with ultrahigh-Q crystalline microresonators. *Phys. Rev. A* **82,** 031804(R) (2010).
9. Ding, L. *et al.* Wavelength-sized GaAs optomechanical resonators with gigahertz frequency. *Appl. Phys. Lett.* **98,** 113108 (2011).
10. Zhang, M., Luiz, G., Shah, S., Wiederhecker, G. & Lipson, M. Eliminating anchor loss in optomechanical resonators using elastic wave interference. *Appl. Phys. Lett.* **105,** 051904 (2014).
11. Thompson, J. D. *et al.* Strong dispersive coupling of a high-finesse cavity to a micromechanical membrane. *Nature* **452,** 72–75 (2008).
12. Chan, J., Eichenfield, M., Camacho, R. & Painter, O. Optical and mechanical design of a 'zipper' photonic crystal optomechanical cavity. *Opt. Express* **17,** 3802–3817 (2009).
13. Brooks, D. W. C. *et al.* Non-classical light generated by quantum-noise-driven cavity optomechanics. *Nature* **488,** 476–480 (2012).
14. Rabl, P. Photon blockade effect in optomechanical systems. *Phys. Rev. Lett.* **107,** 063601 (2011).
15. Braginsky, V. B. & Manukin, A. B. *Measurement of Weak Forces in Physics Experiments* (Univ. Chicago Press, 1977).
16. Gavartin, E., Verlot, P. & Kippenberg, T. J. A hybrid on-chip optomechanical transducer for ultrasensitive force measurements. *Nature Nanotech.* **7,** 509–514 (2012).
17. Grudinin, I. S., Lee, H., Painter, O. & Vahala, K. J. Phonon laser action in a tunable two-level system. *Phys. Rev. Lett.* **104,** 083901 (2010).
18. Mahboob, I., Nishiguchi, K., Fujiwara, A. & Yamaguchi, H. Phonon lasing in an electromechanical resonator. *Phys. Rev. Lett.* **110,** 127202 (2013).
19. Jing, H. *et al.* PT-symmetric phonon laser. *Phys. Rev. Lett.* **113,** 053604 (2014).
20. Chan, J. *et al.* Laser cooling of a nanomechanical oscillator into its quantum ground state. *Nature* **478,** 89–92 (2011).
21. Teufel, J. D. *et al.* Sideband cooling of micromechanical motion to the quantum ground state. *Nature* **475,** 359–363 (2011).
22. O'Connell, A. D. *et al.* Quantum ground state and single-phonon control of a mechanical resonator. *Nature* **464,** 697–703 (2010).
23. Sciamanna, M. & Shore, K. A. Physics and applications of laser diode chaos. *Nature Photon.* **9,** 151–162 (2015).
24. Uchida, A. *et al.* Fast physical random bit generation with chaotic semiconductor lasers. *Nature Photon.* **2,** 728–732 (2008).
25. Redding, B. *et al.* Low spatial coherence electrically pumped semiconductor laser for speckle-free full-field imaging. *Proc. Natl Acad. Sci. USA* **112,** 1304–1309 (2015).
26. Gammaitoni, L., Hänggi, P., Jung, P. & Marchesoni, F. Stochastic resonance. *Rev. Mod. Phys.* **70,** 223–287 (1998).
27. McDonnell, M. D. & Abbott, D. What is stochastic resonance? Definitions, misconceptions, debates, and its relevance to biology. *PLoS Comput. Biol.* **5,** e1000348 (2009).
28. Gang, H., Ditzinger, T., Ning, C. Z. & Haken, H. Stochastic resonance without external periodic force. *Phys. Rev. Lett.* **71,** 807 (1993).
29. McDonnell, M. D. & Ward, L. M. The benefits of noise in neural systems: bridging theory and experiment. *Nature Rev. Neurosci.* **12,** 415–426 (2011).
30. Anishchenko, V. S., Neiman, A. B. & Safanova, M. A. Stochastic resonance in chaotic systems. *J. Stat. Phys.* **70,** 183–196 (1993).
31. Mantegna, R. N. & Spagnolo, B. Stochastic resonance in a tunnel diode. *Phys. Rev. E* **49,** R1792–R1795 (1994).
32. Rouse, R., Han, S., & Lukens, J. E. Flux amplification using stochastic superconducting quantum interference devices. *Appl. Phys. Lett.* **66,** 108–110 (1995).
33. Hänggi, P. Stochastic resonance in biology how noise can enhance detection of weak signals and help improve biological information processing. *ChemPhysChem.* **3,** 285–290 (2002).
34. Badzey, R. L. & Mohanty, P. Coherent signal amplification in bistable nanomechanical oscillators by stochastic resonance. *Nature* **437,** 995–998 (2005).
35. McNamara, B., Wiesenfeld, K. & Roy, R. Observation of stochastic resonance in a ring laser. *Phys. Rev. Lett.* **60,** 2626–2629 (1988).
36. Gammaitoni, L., Marchesoni, F., Menichella-Saetta, E. & Santucci, S. Stochastic resonance in bistable systems. *Phy. Rev. Lett.* **62,** 349–352 (1989).
37. Abbaspour, H., Trebaol, S., Portella-Oberli, M. & Deveaud, B. Stochastic resonance in collective exciton–polariton excitations inside a GaAs microcavity. *Phys. Rev. Lett.* **113,** 057401 (2014).
38. Liu, Z. & Lai, Y.-C. Coherence resonance in coupled chaotic oscillators. *Phys. Rev. Lett.* **86,** 4737–4740 (2001).
39. Karsaklian Dal Bosco, A., Wolfersberger, D. & Sciamanna, M. Delay-induced deterministic resonance of chaotic dynamics. *Euro. Phys. Lett.* **101,** 24001 (2013).
40. Masoller, C. Noise-induced resonance in delayed feedback systems. *Phys. Rev. Lett.* **88,** 034102 (2002).
41. Arteaga, M. A. *et al.* Experimental evidence of coherence resonance in a time-delayed bistable system. *Phys. Rev. Lett.* **99,** 023903 (2007).
42. Pikovsky, A. S. & Kurths, J. Coherence resonance in a noise-driven excitable system. *Phys. Rev. Lett.* **78,** 775–778 (1997).
43. Neiman, A., Saparin, P. I. & Stone, L. Coherence resonance at noisy precursors of bifurcations in nonlinear dynamical systems. *Phys. Rev. E* **56,** 270–273 (1997).
44. Lindner, B. & Schimansky-Geier, L. Analytical approach to the stochastic FitzHugh–Nagumo system and coherence resonance. *Phys. Rev. E* **60,** 7270–7276 (1999).
45. Postnov, D. E., Han, S. K., Yim, T. G. & Sosnovtseva, O. V. Experimental observation of coherence resonance in cascaded excitable systems. *Phys. Rev. E* **59,** R3791–R3794 (1999).
46. Ilchenko, V. S. & Gorodetskii, M. L. Thermal nonlinear effects in optical whispering gallery microresonators. *Laser Phys.* **2,** 1004–1009 (1992).
47. Carmon, T., Yang, L. & Vahala, K. J. Dynamical thermal behavior and thermal self-stability of microcavities. *Opt. Express* **12,** 4742–4750 (2004).
48. Carmon, T., Cross, M. C. & Vahala, K. J. Chaotic quivering of micron-scaled on-chip resonators excited by centrifugal optical pressure. *Phys. Rev. Lett.* **98,** 167203 (2007).
49. Bakemeier, L., Alvermann, A. & Fehske, H. Route to chaos in optomechanics. *Phys. Rev. Lett.* **114,** 013601 (2015).
50. Marquardt, F. & Girvin, S. M. Trend: optomechanics. *Physics* **2,** 40 (2009).
51. Lemarchand, A., Gorecki, J., Gorecki, A. & Nowakows, B. Temperature-driven coherence resonance and stochastic resonance in a thermochemical system. *Phys. Rev. E* **89,** 022916 (2014).
52. Dunn, T., Wenzler, J. & Mohanty, P. Anharmonic modal coupling in a bulk micromechanical resonator. *Appl. Phys. Lett.* **97,** 123109 (2010).
53. Gaidarzhy, A., Dorignac, J., Zolfagharkhani, G., Imboden, M. & Mohanty, P. Energy measurement in nonlinearly coupled nanomechanical modes. *Appl. Phys. Lett.* **98,** 264106 (2011).

Acknowledgements

The authors thank F. Marchesoni for discussions and for interpreting the results on stochastic resonance. Ş.K.Ö. thanks J. Mateo for support. L.Y. and Ş.K.Ö. are supported by ARO grant no. W911NF-12-1-0026. J.Z. is supported by the NSFC under grants nos. 61174084 and 61134008. Y.X.L. is supported by the NSFC under grant no. 61025022. Y.X.L. and J.Z. are supported by the National Basic Research Program of China (973 Program) under grant no. 2014CB921401, the NSFC under grant no. 61328502, the

Tsinghua University Initiative Scientific Research Program and the Tsinghua National Laboratory for Information Science and Technology (TNList) Cross-discipline Foundation. F.N. is partially supported by the RIKEN iTHES Project, MURI Center for Dynamic Magneto-Optics, via AFOSR award no. FA9550-14-1-0040 and a Grant-in-Aid for Scientific Research (A). F.B. is supported by the NSFC under grant no. 11374165 and the 973 Program under grant no. 2013CB328702. The authors thank Z. Shen for helping with the numerical simulations used in the Supplementary Information.

Author contributions

F.M., J.Z. and Ş.K.Ö. contributed equally to this work. J.Z. and Ş.K.Ö. conceived the idea, J.Z. provided theoretical analysis under the guidance of Ş.K.Ö., Y.-x.L. and F.N. Ş.K.Ö. and L.Y. designed the experiments. F.M., J.Z. and B.P. performed the experiments and processed the data with help from Ş.K.Ö. and F.B. J.Z. and Ş.K.Ö. wrote the manuscript with contributions from all authors.

Additional information

Supplementary information is available in the online version of the paper. Reprints and permissions information is available online at www.nature.com/reprints. Correspondence and requests for materials should be addressed to Ş.K.Ö., J.Z. and L.Y.

Competing financial interests

The authors declare no competing financial interests.